Context-Related Frequency Modulations of Macaque Motor Cortical LFP Beta Oscillations

Bjørg Kilavik, Adrian Ponce-Alvarez, Romain Trachel, Joachim Confais, Sylvain Takerkart, Alexa Riehle

Cerebral Cortex September 2012;22:2148–2159
doi:10.1093/cercor/bhr299
Advance Access publication October 20, 2011

Context-Related Frequency Modulations of Macaque Motor Cortical LFP Beta Oscillations

Bjørg Elisabeth Kilavik[1], Adrián Ponce-Alvarez[1], Romain Trachel[1,2], Joachim Confais[1], Sylvain Takerkart[1] and Alexa Riehle[1]

[1]Institut de Neurosciences Cognitives de la Méditerranée, CNRS—Aix-Marseille University, 13402 Marseille Cedex 20, France and [2]Athena Project Team, INRIA Sophia Antipolis—Méditerranée, BP 93 06902 Sophia Antipolis Cedex, France

Address correspondence to Dr Bjørg Elisabeth Kilavik. Email: kilavik@incm.cnrs-mrs.fr.

The local field potential (LFP) is a population measure, mainly reflecting local synaptic activity. Beta oscillations (12–40 Hz) occur in motor cortical LFPs, but their functional relevance remains controversial. Power modulation studies have related beta oscillations to a "resting" motor cortex, postural maintenance, attention, sensorimotor binding and planning. Frequency modulations were largely overlooked. We here describe context-related beta frequency modulations in motor cortical LFPs. Two monkeys performed a reaching task with 2 delays. The first delay demanded attention in time in expectation of the visual spatial cue, whereas the second delay involved visuomotor integration and movement preparation. The frequency in 2 beta bands (around 20 and 30 Hz) was systematically 2–5 Hz lower during cue expectancy than during visuomotor integration and preparation. Furthermore, the frequency was directionally selective during preparation, with about 3 Hz difference between preferred and nonpreferred directions. Direction decoding with frequency gave similar accuracy as with beta power, and decoding accuracy improved significantly when combining power and frequency, suggesting that frequency might provide an additional signal for brain–machine interfaces. In conclusion, multiple beta bands coexist in motor cortex, and frequency modulations within each band are as behaviorally meaningful as power modulations, reflecting the changing behavioral context and the movement direction during preparation.

Keywords: beta oscillations, frequency modulations, local field potential, macaque, motor cortex

Introduction

The local field potential (LFP) is a population measure that mainly reflects the local synaptic activity, with contributions from spike after-potentials and intrinsic transmembrane current changes (Mitzdorf 1985; Logothetis et al. 2007). In the motor cortical LFP, oscillations are often observed, predominantly in the beta range (e.g., 12–40 Hz). These oscillations were associated with several phenomena, ranging from reflecting a "resting" motor cortex (Jasper and Penfield 1949; Pfurtscheller et al. 1996), underlying efficient motor maintenance (Conway et al. 1995; Baker et al. 1999; Kristeva et al. 2007) or more generally the maintenance of the "status quo" (Engel and Fries 2010) to reflecting attention (Gross et al. 2004), sensorimotor binding, and motor planning (Murthy and Fetz 1992, 1996; Sanes and Donoghue 1993; Donoghue et al. 1998; Saleh et al. 2010). Supporting the notion that beta oscillations might reflect sensorimotor binding and motor planning, it was shown that the beta power is selective for movement type both in motor (Heldman et al. 2006; O'Leary and Hatsopoulos 2006; Spinks et al. 2008) and parietal (Scherberger et al. 2005; Asher et al. 2007) cortices.

In this study, we address a subject so far largely neglected. Beta oscillations were typically found to vary in peak frequency, both when comparing subjects participating in the same study (e.g., Donoghue et al. 1998) as well as when comparing different studies (i.e., different behavioral contexts). It is difficult to assess from the literature whether beta oscillations change in frequency in relation to different behavioral contexts or whether interstudy differences mainly reflect intersubject differences. In fact, whereas extensive work was conducted on amplitude modulations of motor cortical oscillations, systematic studies of frequency modulations within a specific band are scarce.

A few studies exist on stimulus-specific frequency modulations of oscillatory activity in monkey primary visual cortex (Gieselmann and Thiele 2008; Feng et al. 2010; Ray and Maunsell 2010). Frequency modulations were also observed during a finger movement task in the subthalamic nucleus of Parkinson's patients (Foffani et al. 2005), but the effects varied from patient to patient. In the human sensorimotor cortex, a small decrease in beta frequency was observed after benzodiazepine intake (Jensen et al. 2005). Finally, regarding monkey motor cortex, reports on differences in beta frequency in different behavioral contexts exist, but systematic quantifications were not made (Murthy and Fetz 1992, 1996; Sanes and Donoghue 1993). Thus, a thorough assessment of context-related frequency modulations of beta oscillations is lacking. In addition, the directional selectivity of the beta frequency was never studied.

We decided to tackle these issues by introducing several distinct behavioral contexts in the same task, sequentially presented within each trial. This allowed us to study within-subject modulations in beta frequency as the behavioral context changed. We trained 2 monkeys in a reaching task that contained 2 delays. The first delay demanded attention in time (i.e., temporal expectation, Coull and Nobre 2008) for the brief presentation of the visual spatial cue (SC). The second was a classical preparatory delay, involving visuomotor integration and movement preparation in 1 of 6 possible directions. Motor cortical oscillations were strong in a low (LO; about 20 Hz) and a high (HI; about 30 Hz) beta band, with context-related modulations in frequency and power within each band. The beta frequency was also directionally selective during movement preparation, permitting movement direction decoding with similar accuracy as when using beta power. In conclusion, frequency modulations were found to be as systematic and behaviorally meaningful as power modulations. We therefore suggest that the context-related analyses of peak frequency values may aid the quest for understanding the possible functional relevance of brain oscillations.

Preliminary results were presented (Kilavik and Riehle 2010).

Materials and Methods

Animal Preparation

Two adult male Rhesus monkeys (T and M, both 9 kg) participated in this study. Care and treatment of the animals during all stages of the experiments conformed to the European and French Government Regulations.

A detailed description of animal preparation and the behavioral task was given in Kilavik et al. (2010) and is briefly outlined here. After learning the task, the monkeys were prepared for multielectrode recordings in the right hemisphere of the motor cortex, contralateral to the trained arm. The chamber locations above motor cortex were verified with T_1-weighted MRI scans in both monkeys, and intracortical microstimulation allowed further subdivision into M1 and PMd in monkey M (see details in Kilavik et al. 2010). Locations in which microstimulation <20 μA current induced muscle twitches were defined as M1. Other locations, where higher current was needed were denoted PMd. Twitches could also be evoked at the most anterior recording locations, indicating we remained within the caudal part of PMd. The recording depths (less than 2 mm below the dura) suggested that we recorded from the rostral part of M1 in the precentral gyrus and not in the anterior bank of the central sulcus. The different recording locations spanned a diameter of about 4 and 13 mm on the surface in monkeys T and M, respectively.

A multielectrode computer-controlled microdrive (MT-EPS, AlphaOmega, Nazareth Illith, Israel) was used to transdurally insert up to 4 or 8 (in monkey T and M, respectively) microelectrodes. Signals were amplified, band-pass filtered from 1 to 250 Hz to obtain the low-frequency LFP signal and stored with a temporal resolution of 1 kHz, along with the behavior that was transmitted online to AlphaMap (AlphaOmega) from the CORTEX software (NIMH, http://www.cortex.salk.edu), which was used to control the task.

Behavioral Task

We trained the monkeys in a two-delay center-out task to make arm movements in 6 directions in the horizontal plane, from a common center position (in some sessions only 2 opposite directions were used, comprising 25% of the LFPs for monkey T and 41% for monkey M). The monkey had continuous visual feedback about hand (cursor) and target positions (red outlines).

Two delays were presented successively in each trial (Fig. 1*A*), the first (D1) demanding temporal attention in anticipation of the visual SC and the second (D2) involving visuomotor integration and movement preparation while waiting for the GO signal. Delay duration (short or long) was modulated from trial to trial in a pseudorandom fashion, but kept the same for both delays within one trial. The short and long delay durations were set to 700 and 1500 ms for monkey T, 1000 and 2000 ms for monkey M. The monkey started each trial by moving the handle to the center and holding it there for 700 ms until a temporal cue (TC) was presented. TC consisted of a 200-ms long tone, its pitch indicating the delay duration to be estimated, starting at the end of the tone (low pitch for short and high pitch for long delay duration). For monkey M, 1 of 2 visual cues was simultaneously presented centrally on the monitor. Neither of the 2 animals had visual/auditory evoked potentials to TC in the LFP (Kilavik et al. 2010), suggesting that TC was encoded/used in motor cortex in a similar way in the 2 monkeys, despite the difference in the sensory modalities of the cue (auditory only vs. combined auditory and visual).

The delay (D1) that followed TC demanded attention in time (i.e., temporal expectation, Coull and Nobre 2008), in order to perceive SC (light-emitting diode [LED]) that was presented very briefly at the end of the delay at the peripheral target location. SC was masked after only 55 ms by the additional illumination of the 5 remaining LEDs, marking the start of D2. During D2, the movement direction indicated by the visual cue SC had to be memorized and prepared. All LEDs then went off at the end of D2 (GO signal), indicating to the monkey to perform the movement.

Data Analysis

While the monkeys performed the reaching task we recorded LFPs in motor cortex. We recorded 287 LFPs in monkey T (90 sessions in 37 days) and 759 LFPs in monkey M (151 sessions in 73 days). We selected 191 LFPs (152 including all 6 directions) in monkey T and 630 LFPs (195 from primary motor [M1] and 435 from dorsal premotor [PMd] cortex; 369 including all 6 directions) in monkey M for further analysis. The remaining LFPs were excluded because of too many artifacts. In the selected LFPs, some trials with obvious artifacts (mainly due to teeth grinding or static electricity), detected by visual inspection, were excluded from further analysis (less than 5% of all trials). The analyzed LFPs contained at least 10 correct trials in each direction, although typically 20 or more correct trials were available per direction. All selected LFPs were included in all analyses, independent of their strength of beta oscillations, but they all had

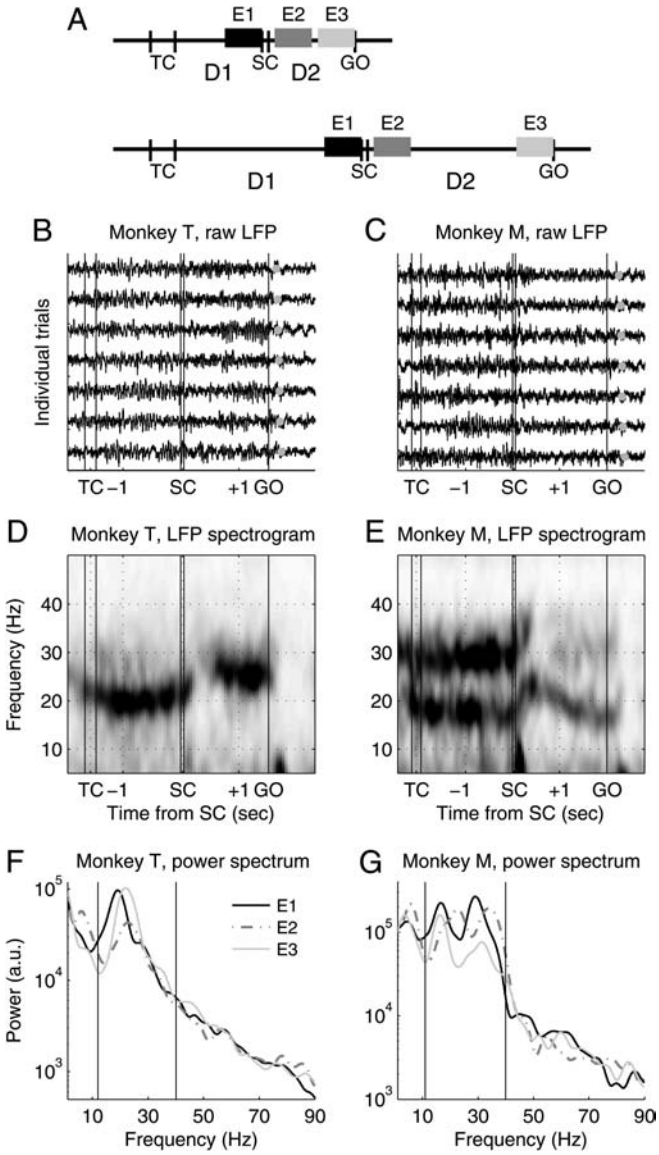

Figure 1. Behavioral task and raw data. (*A*) Task design indicating the time of occurrence of task events in short (on top) and long delay trials. The vertical lines (also in plots *B*–*E*) indicate the onsets or offsets of the task cues. Delay 1, D1; delay 2, D2; go-signal, GO. The task epochs selected for statistical analysis are shown as boxes (E1, E2, and E3). (*B*, *C*) Examples of single-trial raw LFP traces for each monkey, showing several long-delay trials in one movement direction from one LFP. Light gray discs after GO indicate the time of movement onset. (*D*, *E*) Spectrograms for all correct trials in the same LFPs and conditions as shown above. Frequency is on the vertical axis and time along the horizontal axis. Darker gray indicates increased power (a.u.). (*F*, *G*) Power spectra for all correct trials in the same LFPs and conditions during 3 different trial epochs (epochs E1, E2, and E3; see *A*). The vertical lines indicate the region of analysis (12–40 Hz).

increased power within the beta range, visible in the spectrograms. In the results, we group LFPs from M1 and PMd since no significant differences were observed between the 2 data sets.

All analyses were conducted offline by using Matlab (The MathWorks Inc.). In the following, the abbreviation LFP refers to the LFP signal recorded on one electrode during one experimental session. We determined the peak frequency and power between 12 and 40 Hz in a time-resolved manner by making power spectral density analyses in 300-ms sliding windows (50-ms steps) for all correct trials for each LFP. We used the pwelch function in Matlab, based on Welch's method, which windows the data with a hamming window. We analyzed with frequency intervals of 0.1 Hz (i.e., high-density spectrum, implemented by zero-padding the data), and the data in each 300-ms sliding window were analyzed as one section (i.e., not using the default mode of the pwelch function that splits the data in multiple partly overlapping sections). In the figures, the averages in each sliding window across all trials or LFPs were plotted at the center of each window (Fig. 1*D*,*E* and Figs 3–5). For each trial and window position, we determined the peak frequency, that is, the frequency with the highest (peak) power between 12 and 40 Hz. Before averaging across LFPs, for each LFP, we normalized the single-trial peak power values for all 300-ms sliding windows, by dividing by the mean power between 12 and 40 Hz (Fig. 2*C*,*D* and Fig. 3).

For statistical analysis on power and frequency modulations related to the behavioral contexts in the different task epochs, we used the single-trial peak power and frequency estimates in each LFP. We selected 3 task epochs (black—light gray boxes in Fig. 1*A*). These epochs were E1: the last 300 ms of D1; E2: 100–400 ms after SC onset; E3: −350 to −50 ms before the GO signal. These epochs contained the 3 different behavioral (cognitive) contexts of the task: attention in time (awaiting the visual SC) during D1 (epoch E1); visuomotor integration after SC in D2 (epoch E2); movement preparation before GO in D2 (epoch E3).

We started by estimating the peak beta frequency (i.e., the frequency with maximal power) in a broad frequency range between 12 and 40 Hz (Fig. 2) across all single trials in all LFPs in both monkeys. We set the lower limit to 12 Hz to avoid picking up the visual evoked potential (VEP) after SC (see examples with increased power below 10 Hz in Fig. 1*D*,*E*, and see Kilavik et al. 2010). In monkey M, 2 beta bands were strong, so all further analysis was made by separating this broad range into 2 narrower, between 12 and 25 Hz (LO band) and 25 and 40 Hz (HI band). In monkey T, there was a clearly dominant LO-band, with a weaker HI-band less well separated from the LO band (Fig. 2*A*,*C*). We therefore analyzed quantitatively only the LO-band between 12 and 40 Hz (cutting at 25 Hz would have compromised too much the LO band, as it had higher frequencies than the LO band in monkey M, see Fig. 2).

Statistical comparisons between the different task epochs were made with analyses of variance (ANOVAs), including also the factors delay duration and movement direction whenever appropriate. Correlation

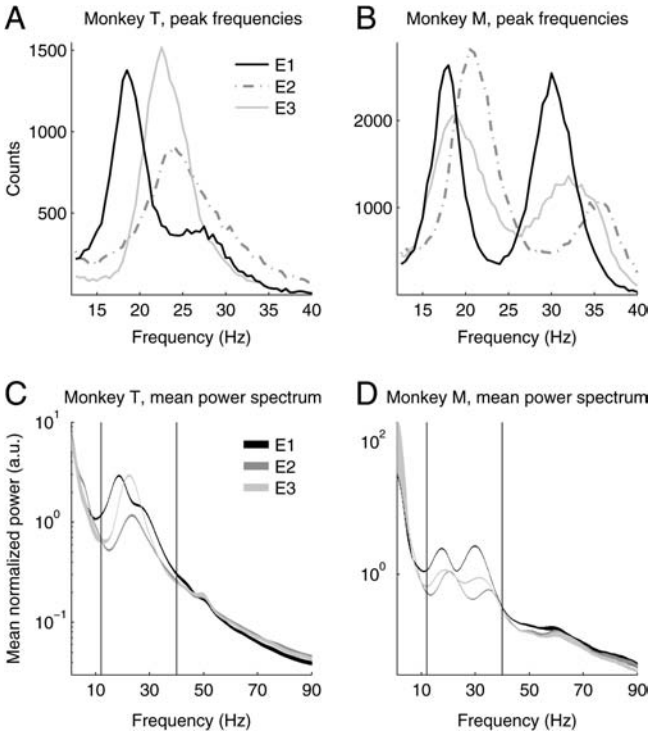

Figure 2. Peak frequency distributions and mean power spectra. (*A*, *B*) Distributions of single trial peak beta frequencies between 12 and 40 Hz for all short trials in all LFPs in each monkey (n = 21 687 and 57 939 in monkey T and M, respectively), estimated in 3 different task epochs (E1 before SC, E2 after SC, and E3 before GO; see Fig. 1*A*). The time–frequency analysis was done with 0.1 Hz frequency intervals (see Materials and Methods), but data are presented here with 0.5 Hz steps. (*C*, *D*) The mean normalized power spectra across all LFPs (short trials) for each monkey, calculated in 3 trial epochs (E1, E2, and E3). The thickness of the curves represent ±standard error. Before spectral analysis, each LFP was treated offline with a narrow 50-Hz "notch" filter (8th order Butterworth band-stop filter with stop band 49.9–50.1 Hz), and the power spectra for each LFP was normalized to the mean power across all epochs between 12 and 40 Hz. The vertical lines indicate the region of analysis (12–40 Hz), corresponding to the complete span of the *x*-axes in the plots in *A*, *B*.

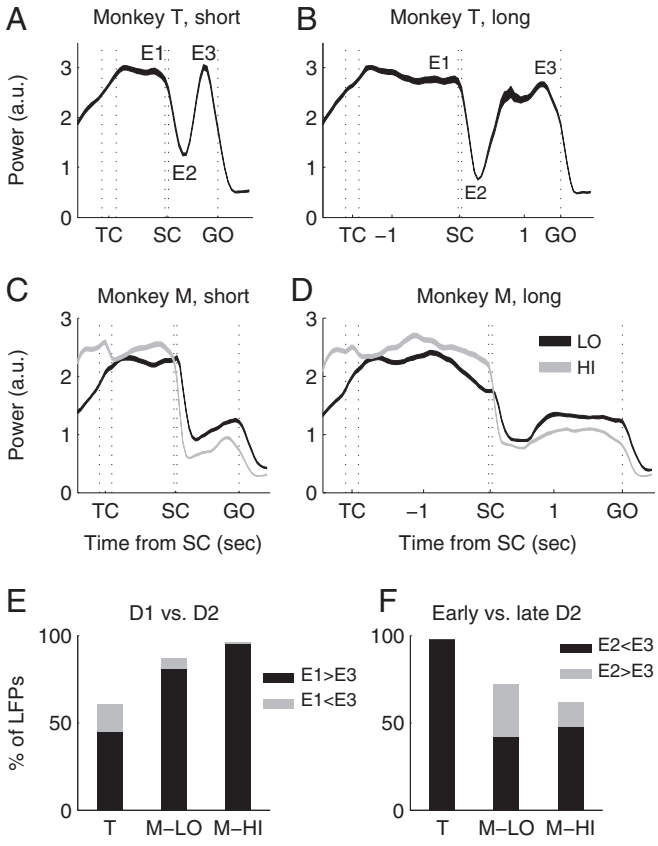

Figure 3. Context-related power modulations. (*A*–*D*) Time-resolved beta power averaged across all LFPs, short delay trials at the left, and long delay trials at the right, monkey T on top. The curves represent the mean normalized peak power estimates (±standard error). The trial epochs used for statistical analysis are marked in the curves for monkey T. (*E*) Percentages of LFPs with significant differences in peak power, comparing activity in D1 with the activity before GO in D2 (epochs E1 vs. E3), for the LO band in monkey T (T) and the LO and HI bands in monkey M (M-LO and M-HI, respectively). The proportions in black have significantly higher power in E1 compared with E3 and gray proportions are those with a significant effect in the opposite direction. (*F*) Percent of LFPs with significant differences in peak power comparing activity after SC with activity before GO (epochs E2 vs. E3 in D2). The proportions in black have significantly higher power in E3 compared with E2, gray shows the proportions with a significant opposite effect. In *E* and *F*, the significance of power differences in each LFP was estimated with a 3-way ANOVA, with delay duration (short and long), movement direction (2 or 6, depending on session), and epoch (E1 vs. E3 or E2 vs. E3) as factors.

tests were made with Spearman's rank correlation test. Chi-square tests were used to compare proportions with significant effects in different groups. The Wilcoxon–Mann–Whitney rank sum test was used to compare distributions of differences in preferred directions. For all statistical tests, the significance threshold was set at $P = 0.05$, unless otherwise stated.

Directional selectivity of peak beta frequency and power was determined using single-trial values before GO, for the LFPs recorded in sessions including all 6 directions ($n = 152$ and 369 in monkeys T and M, respectively). For improved single-trial peak power and frequency estimates, we used the final 500 ms before GO, including three 300 ms sections with 200-ms overlap for the pwelch analysis. The "preferred direction" was defined as the direction of the vector sum of the mean frequency or power estimates in the 6 directions, thus arbitrarily defined as the direction with the highest frequency or power, respectively. We determined the significance of the directional selectivity using a resampling procedure (see Kilavik et al. 2010). In this procedure, the length of the vector sum was taken as the strength of directional selectivity. For each LFP, single-trial frequency (or power) estimates were then randomly reassigned to 1 of the 6 movement directions, and a new vector sum was calculated. This procedure was repeated 1000 times, and the length of the vector sum of the original data was compared with the vector sums of the resampled data. If the original vector sum was larger than 950 of the 1000 resampled vector sums ($P < 0.05$), the beta frequency (or power) in that LFP was deemed directionally selective.

Circular statistics were made in part by using the circular statistics toolbox for Matlab (Berens 2009). Nonuniformity of the population distributions of preferred directions were made with the Hodges–Ajne test, which is efficient also if the underlying distributions are bimodal or multimodal (Berens 2009). We measured the angular deviation of each distribution (Berens 2009), which is a measure of dispersion, defined as $\sqrt{(2(1-R))}$, where R is the mean resultant vector. The angular deviation is bound between $[0\ \sqrt{2}]$. We additionally compared the dispersions of the different distributions by comparing the distributions of angular distances of individual data points in each distribution to their mean direction with a Wilcoxon–Mann–Whitney rank sum test (as described in Batschelet 1981). Finally, we estimated whether nonuniform distributions were rather unimodal or bimodal, using an approach which was described and tested in Guerrasio et al. (2010). Note that for bimodal distributions, the mean direction and therefore the angular deviation and the above-described measures of dispersion (calculated using the mean vector length or direction, respectively) do not adequately describe the data. However, in these cases (only one of the distributions was estimated to be rather bimodal), the statistical results from comparisons of the dispersion of this distribution with the other ones corresponded well with direct observations of the data.

To determine how much information there was about the movement direction in the frequency of a given LFP, we computed the mutual information (MuI) between movement direction and frequency, which is given by

$$\mathrm{MuI} = -\sum_{v} P(v)\log_2 P(v) + \sum_{d} P(d)\sum_{v} P(v|d)\log_2 P(v|d), \qquad (1)$$

where d is the movement direction, $P(v|d)$ is the probability of observing the frequency v given the movement direction d, and $P(v)$ is the probability of observing the frequency v across all trials in any movement direction. As the 6 movement direction conditions were presented at random with equal probability, $P(d) = 1/6$. MuI quantifies in units of bits the reduction of uncertainty about the movement direction that can be gained from the observation of the LFP frequency in a single trial. MuI is zero only if the frequency-movement direction relationship is random. The maximum value of MuI equals the entropy of the movement direction, that is, $H(D) = -\sum p(d)\log_2 p(d) = \log_2(6) = 2.585$. The probabilities $P(v)$ and $P(v|d)$ were estimated for each LFP from the empirical data by constructing histograms with the range of frequencies partitioned into bins (bin size being a free parameter in our analysis; see Fig. 6). Due to finite sampling, the probabilities are subject to both systematic error bias and statistical error (variance). To correct for this and to asses MuI values that were significantly different from zero ($P < 0.05$), we randomly associated frequencies and directions (1000 shuffles) to obtain a mean baseline, $\langle \mathrm{MuI}^{sh} \rangle$, and 95% confidence intervals for the empirical mutual information (MuI^{emp}) for each LFP (Panzeri et al. 2007).

To perform an offline decoding analysis of the movement direction on a single-trial basis, we used a homemade software toolbox that performs supervised classification as follows. First, the data are split into a testing and a training subset, containing one- and four-fifths of the trials, respectively. During training, each movement direction is characterized by learning from the LFP observations of the training set to build a decoder. Then, the performance of this decoder (rate of correct decoding) is measured with the remaining trials constituting the testing set. The generalization capability of the method is estimated by a 5-fold cross-validation, that is, by repeating this process on 5 different disjoint training and testing subsets, until the full data set has been browsed in the testing phase. The features used as inputs to the classifier were either the frequency or the power alone or both. The LFPs that were included in this decoding analysis (and subsequent comparisons of preferred directions between different features or LFPs) were selected to present features that were at least slightly directionally selective (a less restrictive criterion of $P < 0.1$ in the directional selectivity analysis described above; selected to have an objective criterion to increase the number of included LFPs) and to have a minimum of 15 correct trials per direction (in order to be able to perform the cross-validation). This provides a feature space of a size equal to the number of included LFPs (when using the frequency or the power alone) or the twice the number of LFPs (when using both features together). For a given subset of N LFPs (*x*-axes in Fig. 7*A–C*), we randomly chose N LFPs among the total set of included ones to perform the entire analysis. We repeated this 50 times in a bootstrap fashion in order to assess the variability of the results. Among the different algorithms available in our toolbox, we only present the results obtained with Learning Vector Quantization (Kohonen 1997), which is a rather simple method previously used on similar data (e.g., Nicolelis et al. 1998); other algorithms produced similar performance levels and no difference in the qualitative nature of the results described here.

Results

Two monkeys were trained in a reaching task containing 2 delays, the first demanding attention in time in anticipation of the cue (SC) and the second involving visuomotor integration and preparation. Monkey T had average success rates of 75% and 69% in short and long trials, respectively, whereas for monkey M, the success rates were 84% and 75%, respectively (less errors in short trials for both monkeys; $P << 0.001$, paired *t*-test across all sessions). About 67% of the errors were directional. The average reaction times were 167 and 210 ms in monkey T and 236 and 257 ms in monkey M, in short and long delay trials, respectively (faster reaction times in short trials in both monkeys; $P << 0.001$ paired *t*-test across all sessions). Time estimation variability increases with delay duration (Gibbon 1977). In addition, the directional information was presented only briefly (55 ms) at the end of a timed interval (700–2000 ms duration). Thus, the directional information had to be kept in working memory during the preparatory delay (also 700–2000 ms duration). These 2 factors (time estimation and retention of directional information) might be the principal reasons for the higher proportions of errors and longer reaction times in long delay trials.

Motor Cortical Beta Oscillations

While the monkeys performed the task, we recorded LFPs in motor cortex. The LFPs of both monkeys contained strong oscillatory activity in the beta-range (12–40 Hz) during long periods of the task, visible in single-trial traces (Fig. 1*B,C*). The example spectrograms (Fig. 1*D,E*) show increased power around 20 Hz (LO) in monkey T and around 18 Hz (LO) and

30 Hz (HI) in monkey M. The power spectra of the same LFPs, estimated in 3 trial epochs (E1, E2, and E3; see Fig. 1*A*), also show one main peak in the beta range in monkey T and 2 peaks in monkey M (Fig. 1*F*,*G*).

Beta oscillations were consistent in frequency across trials and across LFPs recorded from different electrodes and days. The peak frequencies, estimated in all single trials of all recorded LFPs, were narrowly distributed (Fig. 2). We could detect a peak in the beta range (12–40 Hz) in all but 8 individual data segments across all LFPs in the 2 monkeys (of more than 150 000 totally analyzed data segments, including all single trials for epochs E1, E2, and E3). This and the narrow distributions indicate that our method produced reliable estimates of peak frequencies in the different task epochs. Given the 2 clear bands in monkey M, all further analyses were done in 2 separate frequency ranges, between 12 and 25 Hz for the LO band and between 25 and 40 Hz for the HI band. After separating between LO and HI bands in monkey M, we were still able to detect a peak within each of the bands in epochs E1, E2, and E3 in 91% of all single trials. Thus, in most trials, the LO and HI bands were simultaneously present rather than alternating between trials. The peak frequency distribution for monkey T in epoch E1 indicated the presence of an HI band centered at about 27 Hz, although much less prominent than the LO band (Fig. 2*A*). Because the LO and HI bands were less well separated and the LO band was so dominant, we only quantified the LO band in this monkey.

The task epochs after SC (epoch E2) and before GO (epoch E3) had somewhat higher peak frequencies compared with the epoch before SC in both monkeys. The individual (Fig. 1*F*,*G*) and mean (Fig. 2*C*,*D*) power spectra suggest that in each task epoch there was either a single-peaked (LO band; in monkey T) or double-peaked (LO and HI bands; in monkey M) process in the beta range (12–40 Hz), riding on a background process with an inverse relationship between power and frequency ($\sim 1/f$). While the background process remained fairly stable across the different task epochs, the peak frequency in each beta band shifted slightly (see details below).

Figure 3 shows the averaged time-resolved beta power for the LO band in monkey T and the LO and HI bands in monkey M. Beta power was strong during temporal expectation of SC in D1, decreased in power during visuomotor integration after SC, and then increased in power during movement preparation toward the GO signal. Beta power was strongly reduced after GO (significantly less power in the LO and HI bands after GO in 96% of LFPs). Most LFPs had significantly stronger beta power during D1 than in the epoch before GO (45–95%; Fig. 3*E*), although the effect was weaker and more variable in monkey T. Less than 16% had higher power before GO than during D1. An HI band was noticeable in the spectrograms of about 15% of the LFPs in monkey T but only in D1 (see also Fig. 2*A*,*C*). Thus, the HI band in monkey T was also weaker in D2 than in D1. During D2, a majority of LFPs had significantly higher power before GO compared with after SC, although this effect was weaker and more variable in monkey M (42–98% with higher power before GO; less than 30% with higher power after SC; Fig. 3*F*).

Context-Related Modulations of Beta Frequency

The beta frequency varied systematically during the task (Fig. 4). In both monkeys, it was lowest during D1, increased abruptly after SC and then decreased gradually during D2. After GO, the frequency increased again (significant in 41% of LFPs for the LO bands and in 16% for the HI band; overall less than 7% had a lower frequency after GO). The frequency was higher during movement preparation before GO compared with when the monkey awaited the visual cue in D1, a difference which was significant in most LFPs in monkey T (90%) and for the HI band in monkey M (79%; Fig. 4*G*). The frequency of the LO band in monkey M decreased more in D2, on average reaching the pre-SC level around the time of the GO signal (Fig. 4*C*,*D*; only 39% had significantly higher LO band frequency before GO than during D1; still, only 4% had the opposite effect). The frequency of the majority of LFPs during D2 was also significantly higher after SC compared with before GO (51–68%; Fig. 4*H*), and again only a few LFPs had the opposite effect (less than 6%). These systematic

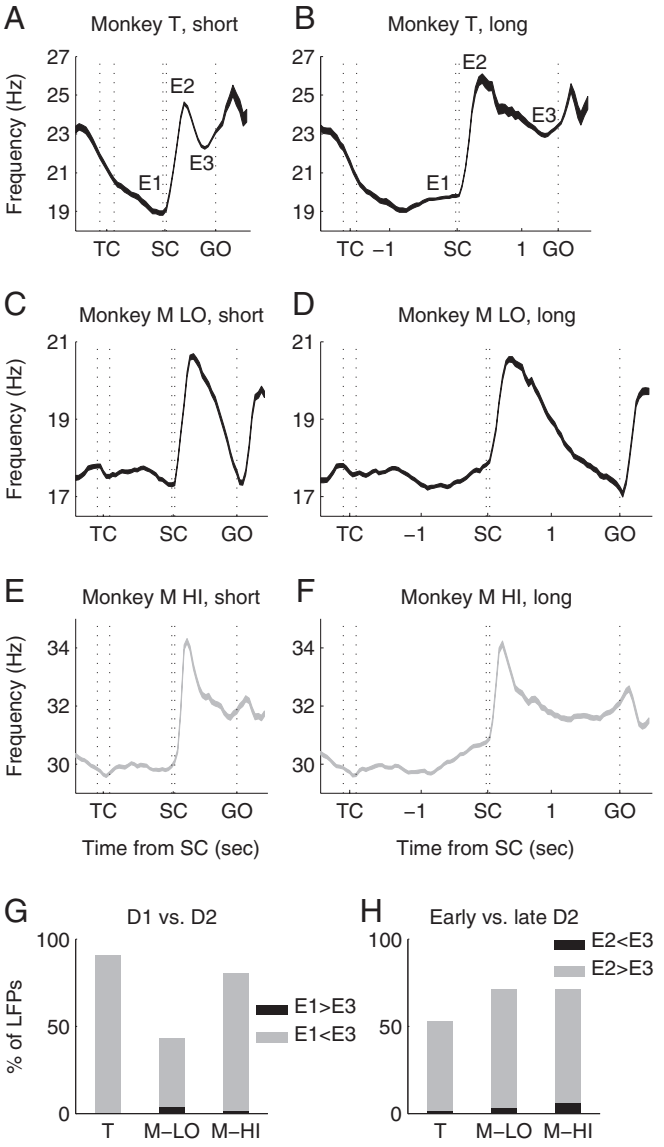

Figure 4. Context-related frequency modulations. (*A*–*F*) The time-resolved beta frequency, averaged for all LFPs in the 2 monkeys, monkey T on the top and monkey M LO and HI in the middle 4 plots. (*G*) Percentages of LFPs with significant differences in peak frequency comparing activity in D1 with the activity before GO in D2 (epochs E1 vs. E3). (*H*) Percentages of LFPs with significant differences in peak frequency comparing activity after SC with activity before GO, in D2 (epochs E2 vs. E3). Details as in Figure 3.

differences in peak frequency in the different task epochs are also evident in the single-trial distributions and the averaged power spectra, shown in Figure 2.

The frequency modulations between different task epochs (Fig. 4*G,H*) were more reliable across LFPs than the power modulations (Fig. 3*E,F*). Whereas almost all LFPs with significant modulations in peak frequency had the same direction of an effect, for example, frequency after SC higher compared with before GO, the power modulations varied more among the different LFPs.

Finally, the peak power and frequency of beta oscillations were significantly negatively correlated trial-by-trial in many LFPs (epoch E1 in short trials: 47% in monkey T, 15% and 68% in monkey M LO and HI, respectively; overall, only 2% with positive correlations; similar results were found in epoch E3).

LO and HI Beta Bands

Monkey M often had 2 beta bands present with similar power (e.g., Fig. 1*E*). Before SC, in epoch E1, there were similar proportions of LFPs with significantly higher power in the LO band than in the HI band (LO band dominance) and vice versa (Table 1). However, there was a larger drop in power from epoch E1 to E3 in the HI band (57%, averaged across all LFPs) compared with the LO band (38%). Thus, the proportion of LFPs with HI band dominance dropped substantially in D2. Similarly, in monkey T, the HI band was only discernible in the frequency distributions and power spectrum in epoch E1 (see Fig. 2*A,C*).

We found similar proportions of HI and LO band dominance in M1 and PMd. However, 60% of the LFPs in monkey M could with certainty be assigned to arm regions by microstimulation effects. The remaining LFPs were either obtained from foot or body regions (11%) or from positions where microstimulation did not evoke responses. In general, the LFPs recorded in these putative nonarm regions were comparable to those recorded in arm regions and were therefore included in this study. But during D1, among the putative "nonarm" LFPs, many more had a significant HI than an LO band dominance (Table 1; significantly more LFPs with HI than LO band dominance in nonarm regions and significantly more HI band dominance in nonarm compared with arm regions, chi-square, $P < 0.01$). In addition, the LO band domination in D2 was weaker in nonarm regions compared with arm regions (Table 1).

Table 1
LO and HI band dominance in monkey M

Data sets \ Epochs	Epoch E1	Epoch E2	Epoch E2
All LFPs (n = 630)	193 LO > HI (31%)	387 LO > HI (61%)**	358 LO > HI (57%)**
	235 LO < HI (37%)	110 LO < HI (17%)	151 LO < HI (24%)
Arm regions	135 LO > HI (36%)	274 LO > HI (72%)**	239 LO > HI (63%)**
(n = 379)	104 LO < HI (27%)	42 LO < HI (11%)	60 LO < HI (16%)
Nonarm regions	58 LO > HI (23%)**	113 LO > HI (45%)*	119 LO > HI (47%)
(n = 251)	131 LO < HI (52%)	68 LO < HI (27%)	91 LO < HI (36%)
M1 (n = 195)	63 LO > HI (32%)	114 LO > HI (58%)**	99 LO > HI (51%)**
	73 LO < HI (37%)	36 LO < HI (18%)	50 LO < HI (26%)
PMd (n = 435)	130 LO > HI (30%)	273 LO > HI (63%)**	259 LO > HI (68%)**
	162 LO < HI (37%)	74 LO < HI (17%)	101 LO < HI (23%)

Note: Differences in LO and HI band power in each LFP was tested with a 2-way ANOVA in D1 (E1; factors: band and delay duration) and with a 3-way ANOVA in D2 (E2 and E3; factors: band, delay duration, and movement direction). Differences in the percentages of LFPs with LO and HI band dominance were determined with chi-square tests, significance levels $P < 0.05$ (*), $P < 0.01$ (**).

Interestingly, the LO and HI bands covaried in frequency and power from trial to trial. About 18% of the LFPs had a significant positive trial-by-trial correlation between LO and HI band power and 25% had a positive trial-by-trial correlation between LO and HI band frequency (less than 1% negative correlations for either power or frequency; epoch E1 in short-delay trials).

Directional Selectivity of Beta Frequency

The beta power is directionally selective during preparation (e.g., Scherberger et al. 2005; O'Leary and Hatsopoulos 2006). However, the selectivity of the beta frequency has never been studied. We therefore analyzed directional selectivity before GO. We found many LFPs to be significantly selective for movement direction either in power or frequency or both. An example of one LFP that was selective for direction in the beta frequency is shown in Figure 5*A*. Overall 24–64% of LFPs were selective in power and 12–49% were selective in frequency in short delay trials, comparable proportions were significant in long delay trials (see numbers in Fig. 5). The average differences in frequency between the preferred and nonpreferred directions across all significant LFPs were 2.4–3.5 Hz (Fig. 5).

The preferred directions were not homogeneously distributed around the circle ($P < 0.01$ for all distributions, Hodges–Ajne test), and all distributions were unimodal, apart from for the HI band power in monkey M, which was estimated to be rather bimodal (with median directions of the 2 modes at 22 and 253°). The distributions had significantly broader dispersion for monkey M than for monkey T. In monkey T, the distribution for power had somewhat larger angular deviation (0.51) than that for frequency (0.42) and the dispersion for power was significantly broader than that for frequency ($P < 0.01$). There was no significant difference in the dispersion of power and frequency for either of the bands in monkey M, and the angular deviations were rather large, ranging between 1.06 and 1.20 for frequency and power in the LO and HI bands (1.11 for the bimodal HI band power distribution). The proportions of tuned LFPs in M1 and PMd in monkey M were the comparable, and the bimodal distribution for HI-band power could not be explained by considering M1 and PMd separately.

Decoding Movement Direction Using Beta Frequency

The beta frequency was directionally selective in a similar proportion of LFPs as was the beta power. This inspired us to further investigate how much information about the movement direction was contained in the beta frequency during preparation. We employed an information theory analysis to calculate, for each LFP, the mutual information (MuI) between LFP frequency and movement direction. Figure 6 shows the averaged MuI for those LFPs that contained significant ($P < 0.05$) information about movement direction, shown for short delay trials. Overall, the amount of information transmitted by single LFPs was relatively small (<0.18 bits). These results indicate that even if a subset of LFPs contain significant amount of information, observing the frequency of one LFP may not be sufficient to predict the animal's intended movement direction in single trials. To compare the amount and reliability of directional information contained in beta frequency and beta power, we decoded movement direction using populations of LFPs and compared the decoding accuracy obtained with either beta frequency or power or by combining both features.

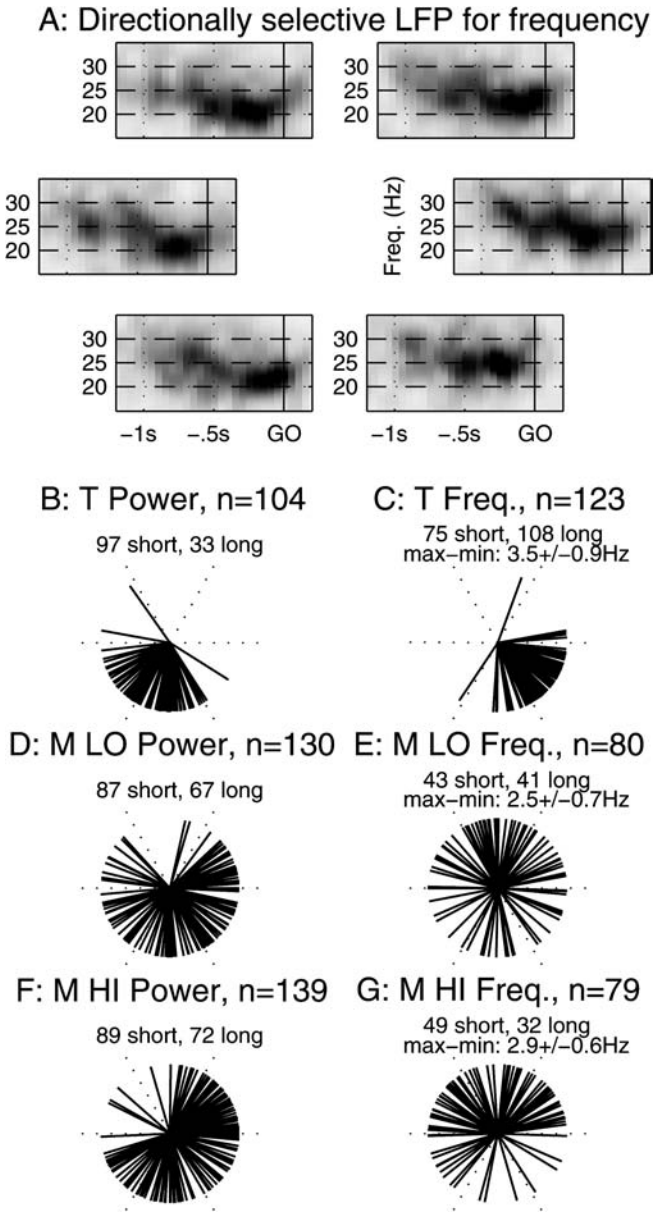

Figure 5. Directional selectivity of beta frequency and power. (*A*) Spectrograms shown for the 6 movement directions of an LFP in monkey T that was significantly directionally selective in peak frequency before GO (vertical lines) in short and long delay trials (only long trials are shown). The average maximal and minimal peak frequencies were 24.4 Hz and 20.3 Hz (toward the lower right and upper left, respectively). Spectrograms are arranged according to the behavioral movement directions. Darker gray indicates increased power (a.u.). (*B–G*) Preferred directions of beta power (left) and frequency (right) of significantly selective LFPs, in monkey T and monkey M LO and HI, from top to bottom. The total number of LFPs used in this analysis was 152 in monkey T and 369 in monkey M (all LFPs that were recorded with 6 movement directions). Within each plot, each line corresponds to one (significantly directionally selective) LFP, pointing in its preferred direction (direction of the vector sum and thus the estimated direction with maximal peak power or frequency). All LFPs that were selective in either short- or long-delay trials were included (*n* in each subfigure title), and only the preferred directions in short trials are shown for LFPs that were directionally selective in both short and long trials. The numbers of significantly selective LFPs in short- and long-delay trials and the average max-min difference in peak frequency for selective LFPs (±standard deviation) are indicated in each subplot. The dotted lines indicate the 6 movement directions.

In order to decode movement direction from a large number of LFPs, we treated our sequentially recorded LFPs as if simultaneously recorded (see, e.g., Scherberger et al. 2005).

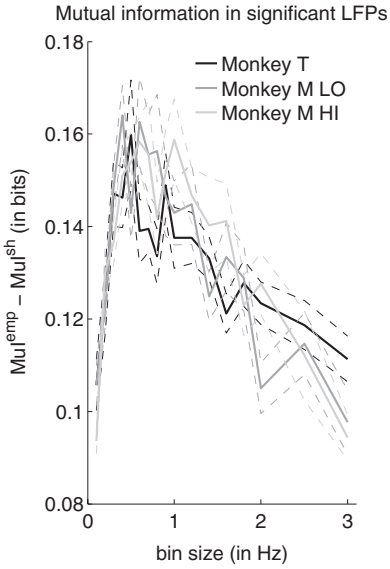

Figure 6. Mutual information between beta frequency and movement direction. Average corrected mutual information ($Mul^{emp} - Mul^{sh}$) between beta frequency and movement direction for all LFPs with significant information in short-delay trials, for different frequency bin sizes. Dashed lines indicate ±standard error. The percentages of LFPs that contained significant information about movement direction, averaged across the different frequency bin sizes, were 30.2%, 9.0%, 7.2% in monkey T and monkey M LO and HI, respectively, corresponding to the average proportions of all 6-direction LFPs that are included in the plot (for each bin size only the LFPs significant for that bin size were included).

Figure 7 shows the decoding performance with varying numbers of LFPs, using only frequency or power, or combining the 2 features, for short delay trials (by using LFPs that were at least weakly directionally selective, $P < 0.1$). In monkey T, the decoding accuracy obtained with beta frequency was the same as that based on beta power, while in monkey M, the decoding was slightly better for power. In addition, by using both features in combination, the decoding performance was significantly improved in both monkeys with respect to that based on either feature in isolation (significantly higher than the best single-feature decoding when using 2 or more LFPs for monkey T; 2 and 3 or more LFPs for monkey M LO and HI, respectively; *t*-test, $P < 0.05$).

Table 2 summarizes the average decoding performance for the maximum number of LFPs available in each data set (corresponding to the maximum number for frequency in monkey T and for frequency and power together in monkey M, see Fig. 7*A*,*C*). We show the results for decoding with twice as many LFPs when decoding only with frequency or power, compared with the combination of both, that is, the size of the total feature space remains the same. This decoding performance was significantly better when combining frequency and power than when using the best single feature for all 3 data sets (*t*-test across 50 bootstraps, $P < 0.01$). For each feature selection, the classification errors were significantly more often assigned to the neighboring targets than to targets which were 2 or 3 steps away.

Comparisons of Preferred Directions

Only some LFPs showed an overlap of power and frequency selectivity and the differences in preferred directions of power and frequency were not systematic in the different bands. Figure 5 already showed that the distributions of preferred

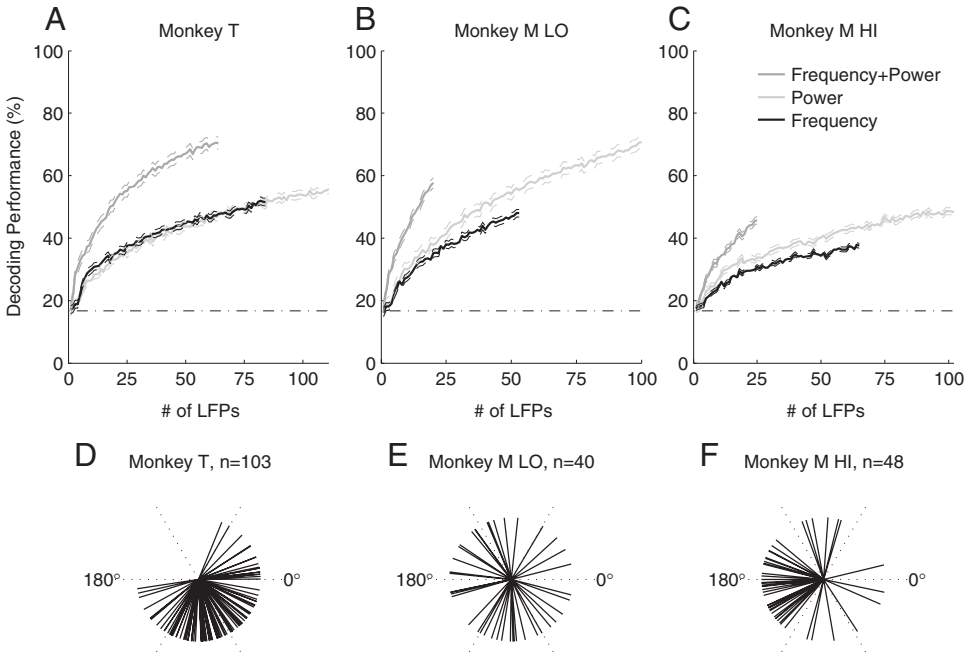

Figure 7. Decoding of movement direction with frequency and power. (*A–C*) Decoding performance (percentages of correctly assigned trials) in short delay trials as a function of the number of included LFPs, using either beta power or frequency or the 2 features combined. Solid lines show the mean decoding performance ±SE (dashed lines; from 50 bootstraps). The black dash-dotted horizontal lines indicate the chance level (16.7%). The maximum numbers of LFPs in the decoding was different for each feature (or feature combination) since we only used LFPs in which the decoded features were at least slightly directionally selective ($P < 0.1$). (*D–F*) Comparison of preferred directions for power and frequency. Only LFPs were included in which power and frequency were both slightly directionally selective ($P < 0.1$), tested separately for short- and long-delay trials. The figures include short and long trials if both were selective (hence the larger *n*'s compared with the maximal numbers of LFPs used for the combined power and frequency decoding, which were only done for short-delay trials). Each line represents one LFP, indicating the angular distance between the preferred directions of power and frequency (zero, to the right, indicates identical preferred directions, 180°, to the left, indicates opposite preferred directions).

Table 2

Decoding performance: Features / Data sets	Power	Frequency	Frequency + power
Monkey T	50.7 ± 1.5% (n = 84)	51.5 ± 1.3% (n = 84)	63.9 ± 1.6% (n = 42)
Monkey M LO	51.4 ± 1.9% (n = 40)	42.7 ± 1.7% (n = 40)	57.7 ± 1.5% (n = 20)
Monkey M HI	40.2 ± 1.7% (n = 50)	34.4 ± 1.6% (n = 50)	45.7 ± 1.5% (n = 25)

Note: Average decoding performance (percent correct ± standard error) for the maximum number of LFPs available in each data set.

directions point in different (but not necessarily opposite) mean directions for power and frequency for each band. To compare preferred directions for power and frequency, we plotted the angular distances between them, for each LFP that was at least weakly directionally selective ($P < 0.1$) for both power and frequency (Fig. 7*D–F*). The preferred directions of power and frequency were about 1 target apart in monkey T (unimodal distribution with a mean at –66° and an angular deviation of 0.82). The distribution was homogeneous around the circle for the LO band in monkey M, but it was centered close to 180° for the HI band, indicating almost opposite preferred directions of power and frequency (unimodal distribution with a mean at –172° and an angular deviation of 0.90).

The preferred directions for the LO and HI bands in monkey M were similar (see Fig. 5), with mean distances of 8 and 21° for power and frequency, respectively (including only LFPs which were at least slightly selective [$P < 0.1$] for LO and HI band power or frequency; unimodal distributions, with an angular deviation of 0.8 and 1.11 for power [$n = 80$] and frequency [$n = 28$], respectively). This similarity in preferred directions is consistent with the positive trial-by-trial correlations between power or frequency of the LO and HI bands.

The similar preferred directions of simultaneously recorded LFPs may be a limitation for the use of oscillations as a brain machine interface (BMI) signal. This was already claimed for the beta power (e.g., Stark and Abeles 2007) but never studied for beta frequency. Since we recorded maximally 4 (monkey T) or 8 (monkey M) LFPs simultaneously, we could not directly decode movement direction using only LFPs recorded in the same session (with so few LFPs the decoding of 6 movement directions does not significantly exceed chance level). We thus decided to compare the differences in preferred directions between pairs of LFPs recorded in 3 different conditions: 1) in the same behavioral session; 2) during the same day but in successive sessions (i.e., with the electrodes being at the same cortical locations but after changing depth; using LFP pairs either from the same or different electrodes); or 3) in different days (i.e., different behavioral sessions, different cortical locations, and different depths). Note that during one recording session, electrodes were placed either relatively close to each other or alternatively in about one-third of the included sessions in monkey M, typically up to 10-mm apart (see Kilavik et al. 2010). Note also that the depths of the different electrodes were independent.

We constructed LFP pairs by combining 2 LFPs that were both at least slightly directionally selective ($P < 0.1$). Each LFP pair was only included in 1 of the 3 populations (same session, same day, or different days), but individual LFPs normally participated in several pairs and in more than one population.

We use only short delay trials, as for the decoding analysis. Figure 8 shows the distributions of differences in preferred directions for the 3 populations. For power and frequency, the differences in preferred directions were smaller for LFPs recorded in the same session than in different days ($P << 0.01$, Wilcoxon–Mann–Whitney rank sum test).

The preferred directions were also more similar for LFPs recorded in the same session than in different sessions in the same day, but the effect was weaker for monkey T ($P = 0.06$ for power and $P = 0.04$ for frequency) than for monkey M ($P < 0.01$ for all comparisons). We subsequently selected the subset of "same day" pairs in which the 2 LFPs were recorded from the same electrode (i.e., same cortical location but different depths and different behavioral sessions). The distributions of differences in preferred directions for these pairs were similar to the complete same day population (not shown). Interestingly, for monkey M's HI band power, there was a large subset of same day LFP pairs with 60–90° difference in preferred direction (see Fig. 8*E*). Most of these LFP pairs belong to one single recording day including 2 successive sessions that formed 36 pairs, combining 6 directionally selective LFPs, whose preferred directions were almost identical in each session (less than 20° apart) but with a clear shift of about 70° for all LFPs from one session to the next (see Fig. 9). Note that the animal's preferred direction (direction with the fastest average reaction time) was the same in the 2 sessions. This example illustrates that, at least in some subjects, the preferred directions may change from one behavioral session to the next, even if the cortical location remains the same (since the cortical depth was also different between electrodes within the same session, this cannot be the main reason for the changes in preferred direction between sessions).

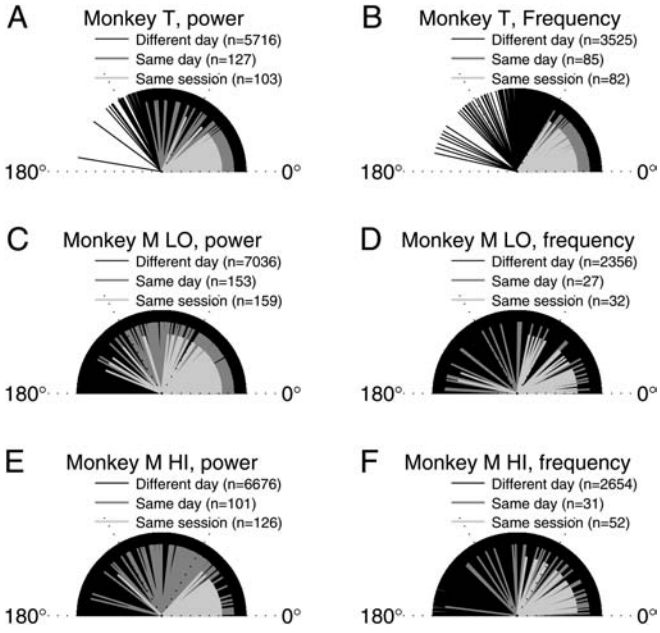

Figure 8. Differences in preferred directions. Distributions of differences in preferred directions between pairs of LFPs recorded either on different electrodes in the same behavioral session, on the same or different electrodes in different sessions in the same day, or in different recording days. The total numbers of pairs for each population are written in the legends. Each line represents one LFP pair, indicating the angular distance between their preferred directions in power (left) or frequency (right), in short-delay trials. Values range from 0° (same preferred directions) to 180° (opposite preferred directions).

At last, to be confident that our results are comparable with more traditional ways of analyzing beta oscillation power, we redid all directional selectivity analyses using the mean power in 10 Hz bands (18–28 Hz for monkey T, 15–25 and 27–37 Hz for monkey M; the bands were selected after visual inspection of the distributions of peak frequencies for epoch E3, in Fig. 2*A,B*). This analysis resulted in an increase of about 5% of significantly directionally selective LFPs, which might be due to reduced noise in the single-trial power estimates. Apart from this, the results remained very similar to those obtained with the peak power. In particular, the mean and clustering of preferred directions remained very similar to the already presented data (see Fig. 5*B,D,F*). In addition, preferred directions remained more similar within the same sessions compared with different sessions in the same day and different days (see Fig. 8*A,C,E*).

Discussion

Multiple beta bands coexist in motor cortex, operating around specific main frequencies. Here, we show for the first time that there are systematic modulations of the peak frequency within each of these bands. The frequency modulations are as reproducible as beta power modulations, concerning the changing behavioral context from cue expectancy to movement preparation and the preparation of arm movements in different directions.

Beta Frequency and Power Modulations

First, it is worth noting that the way we study the beta frequency necessitates a clearly discernible peak in the power spectrum. Beta power modulations are often studied after averaging the power across relatively broad frequency ranges, which does not require a peak in the power spectrum. However, in most cases, the raw data indeed show clear peaks in the beta range (Rickert et al. 2005; Scherberger et al. 2005; O'Leary and Hatsopoulos 2006; Spinks et al. 2008; Saleh et al.

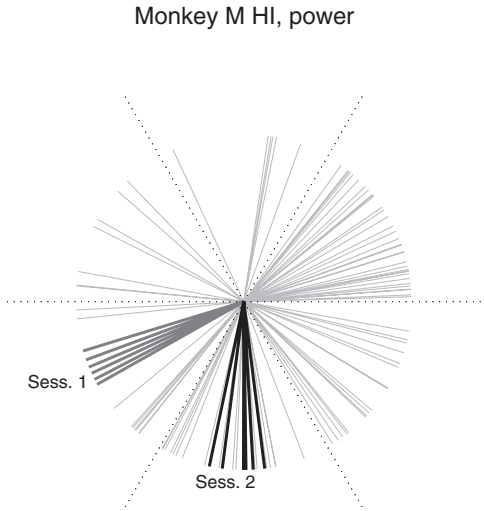

Figure 9. Preferred direction changes within 1 day. Preferred directions of HI band power in monkey M, including all individual LFPs that formed pairs in the same day population. Light gray lines represent all significantly directionally selective LFPs ($P < 0.1$), while dark gray and black lines represent 6 LFPs recorded in 2 different session in the same day (Sessions 1 and 2, respectively). Details as in Figure 5.

2010). We therefore propose that the way we here analyze the data could also be applicable for other data sets involving beta oscillations.

Our task contained several behavioral contexts, which were clearly discernable in the beta power and frequency modulations. Similar to our finding, increased beta power at times when the spatial cue was expected was also found in human motor cortex (Saleh et al. 2010). Thus, increased beta power is at least in part associated with the anticipation of task-relevant sensory cues.

It is not possible to clearly separate visuomotor integration from movement preparation, as, in our task, the 2 processes may partly overlap both in time and space and that in a variable way from trial to trial. This is reflected in the less steep changes in power and frequency during D2, compared with the more abrupt transition around visual cue presentation (SC). Furthermore, we have recently shown that our LFPs have a clear VEP, most prominent about 60–200 ms after SC onset (Kilavik et al. 2010). This is just prior to the minimal power and maximal frequency of the beta oscillations that occurred in the window between 100 and 400 ms after SC onset (epoch E2), but the exact relationship between the VEP and beta modulations remains to be studied. O'Leary and Hatsopoulos (2006) found increased beta power following the onset of the visual cue. The difference between their and our results might be related to an increased urgency to detect and memorize the visual spatial information in our task, as it was available only for 55 ms, compared with the entire preparatory delay in their task.

Beta oscillations were given many roles in motor cortex, on the one hand seen as reflecting a resting motor cortex or maintenance of posture or the status quo (Jasper and Penfield 1949; Pfurtscheller et al. 1996; Baker et al. 1999; Engel and Fries 2010) and, on the other hand, interpreted as reflecting attention or visuomotor integration (Murthy and Fetz 1992; Sanes and Donoghue 1993; Gross et al. 2004; Saleh et al. 2010). The systematic difference that we find in peak frequency (and power) during the different task epochs suggests that beta oscillations reflect multiple processes, including attention (temporal expectation), visuomotor integration, and preparation. Moreover, our data demonstrate that behavioral (cognitive) state transitions are not only discernible in broad-range spectral changes of the LFP (e.g., Scherberger et al. 2005; Hwang and Andersen 2009) but also in systematic frequency modulations within narrow bands. These modulations in motor cortical beta oscillations even reflect state transitions that do not involve overt movements, instead related to the anticipation versus processing of task-relevant sensory cues.

Modulations in the oscillation power has been shown, among others, to reflect the degree of synchronization (Denker et al. 2011) or the overall activity in a set of neurons (Nauhaus et al. 2009) and to be correlated with membrane potential fluctuations of nearby neurons (Poulet and Petersen 2008). However, systematic studies of the oscillation frequency are scarce. In monkey motor cortex, early work suggested modulations in beta frequency in relation to behavior, while lacking systematic quantifications (Murthy and Fetz 1992, 1996; Sanes and Donoghue 1993). Thus, ours is the first systematic study of context-related beta frequency modulations in motor cortex, demonstrating that they are as behaviorally meaningful as power modulations. The particular frequencies of brain oscillations have been linked to interactions between excitation and inhibition (Whittington et al. 2000; Brunel and Wang 2003; Jensen et al. 2005; Buzsaki 2006; Ray and Maunsell 2010). Alternatively, and not incompatible with this, they were suggested to depend on the degree of long-range interactions and bottom-up versus top-down processing (Kopell et al. 2000; von Stein and Sarnthein 2000; Buschman and Miller 2007; Miller 2007). Lower frequencies were associated with interactions in larger and more distributed neuronal assemblies and rather top-down processing (e.g., von Stein and Sarnthein 2000) but also increased inhibition (Jensen et al. 2005). Our data are consistent with the hypothesis that the lower beta frequency in each band, while awaiting the visual cue during D1, reflects more widespread (top-down) networks involved in the temporal expectation to receive movement-related visual information. The weaker power and higher peak frequency during the second delay might reflect the activity of more specific neuronal populations related to either the visual information processing (bottom-up) and/or more local (motor cortical) populations involved in movement preparation. Thus, the systematic frequency modulations suggest that the beta oscillations observed in the different delays reflect, at least in part, different processes.

The negative trial-by-trial (within-epoch) correlation between power and frequency in many LFPs indicates that power and frequency are inversely comodulated. Comparing different task epochs, on average the power tended to be higher in D1, whereas the frequency was higher in D2, consistent with an inverse comodulation. On the other hand, we found no straightforward relationship between the preferred directions of power and frequency (only the HI band in monkey M had close to opposite preferred directions of power and frequency), indicating that frequency and power modulations related to the preparation of different movements may be uncoupled (see below). This suggests that there might be significant information in beta frequency modulations that cannot be deduced directly from the observation of beta power modulations.

Multiple Beta Bands in Motor Cortex

In both animals, the HI band was modulated by the task, being stronger while awaiting the SC during D1 than during movement preparation in D2. In addition, when the HI band was present during preparation, it was selective for movement direction to a similar degree as the LO band. A recent study demonstrated selectivity for grasp type in the beta power in 2 beta bands (LO and HI, about 20 and 35 Hz) in one monkey and in an LO band in another monkey involved in the same motor task (Spinks et al. 2008). However, whereas we found similar preferred directions in the LO and HI bands, they found rather opposite grasp-type selectivity for LO and HI power.

There were many more putative nonarm LFPs with HI-band dominance in D1, while no difference was found between M1 and PMd. This somatotopic relationship is consistent with a few studies in humans relating lower beta frequencies to arm movements and arm regions of sensorimotor cortex and higher beta frequencies to foot movements and foot regions of sensorimotor cortex (Pfurtscheller et al. 2000; Neuper and Pfurtscheller 2001).

Directional Information in Beta Frequency

We found similar proportions of LFPs with frequency and power directional selectivity. This and the lack of a fixed

relationship between the selectivity of power and frequency suggest the use of beta frequency as an additional signal for decoding neuronal activity in the context of BMIs. The beta power of LFPs in parietal (Scherberger et al. 2005; Asher et al. 2007) and motor (Heldman et al. 2006; O'Leary and Hatsopoulos 2006) cortices was already shown to be useful for decoding movement direction during preparation but less so during movement execution (Rickert et al. 2005). We find that the beta frequency provides similar decoding performance as the beta power. In addition, the combined power and frequency decoding, even with only half as many LFPS, gave better results than decoding based on power or frequency alone (see Fig. 7*A–C* and Table 2). This improved decoding performance when using power and frequency together might be due to the rather different preferred directions for the 2 features (see Fig. 7*D–F*).

Note that, we arbitrarily selected the preferred direction for frequency to be the direction with maximal frequency. Whereas one can maybe intuitively imagine how maximal (or minimal) beta power might be "preferred" by the network, it is currently not clear how a slightly higher beta frequency might be more preferable than a lower frequency, whether an intermediate frequency might rather be optimal or whether different frequencies indeed reflect (partly) different neuronal populations participating in the preparation of different movements.

Most LFPs used for decoding were recorded in different sessions. Thus, trial-by-trial correlations between individual LFPs cannot play a major role in limiting the decoding performance in our case. The performance increased as we added LFPs and by combining frequency and power. This was probably due to 2 factors. Increasing the number of decoded features (by increasing the number of LFPs or by combining power and frequency) could increase the signal-to-noise ratio (even if all features would contain identical information but masked by noise). Additionally, it could lead to an effective increase in the total amount of information if different features carried different information, as indeed suggested by the fact that different LFPs (as well as power and frequency) preferred different directions.

However, the similarity in preferred directions of LFPs at different recording sites (see also Scherberger et al. 2005; O'Leary and Hatsopoulos 2006; Asher et al. 2007) and the trial-by-trial correlations were already suggested to be limitations for the usefulness of LFP oscillations in BMIs (e.g., Stark and Abeles 2007), so far only considering the oscillation power. Our analysis suggests that the same restrictions hold for beta frequency since the decoding performance for power and frequency was rather similar. In addition, the dispersion in the distributions of preferred directions for frequency and power were similar. Importantly, for both power and frequency, the preferred directions were more similar for LFPs recorded in the same than in different sessions, both in the same or different days. Thus, the decoding performance in a real BMI situation (with many LFPs in parallel) might be lower than what we find in our analysis, whether or not power and frequency are used simultaneously. The fact that for some subjects the preferred directions might change between different behavioral sessions in the same day suggests that neither beta power nor frequency might provide stable tuning properties for long-term use without the need of recalibrating the decoder. However, the fact that in monkey T, the preferred directions were rather similar, even in different days, suggests that in some subjects the beta power and frequency might indeed provide stable directional information, useful for decoding.

Aside from the relevance for BMI decoding, it is interesting to note, and to our knowledge not yet reported, that the directional selectivity of beta power and frequency can change between successive behavioral sessions in some subjects. This suggests that directional selectivity measured in LFP oscillations is minimally related to the cortical location (and depth). Instead, we speculate that it might rather reflect the current cognitive state of the animal and/or the state of the underlying neuronal network (e.g., balance excitation/inhibition).

Conclusions

We here described systematic LFP beta frequency modulations in monkey motor cortex. These frequency modulations are clearly as meaningful as beta power modulations, both regarding the change of the behavioral context and regarding the movement direction during preparation. Modulations in the oscillation power can be interpreted as reflecting the degree of synchronization or overall activity in a fixed set of neurons or changes in the number of contributing neurons. However, the oscillation frequency may be related to aspects such as network extent, bottom-up versus top-down processes or excitation/inhibition balance, thus suggesting that oscillations at different frequencies indeed reflect different neuronal populations or processes. We therefore suggest that combined studies of frequency and power changes of oscillations will provide more information regarding the differentiation of different neuronal processes giving rise to them and their possible functional roles.

Funding

Agence National de la Recherche (grant ANR-NEUR-05-045-1); AXA Research Fund and Fondation pour la Recherche Médicale (grants to B.E.K.); Consejo Nacional de Ciencia y Tecnología de México (Mexican government) (grant to A.P.-A.); Ministère Recherche et Technologie (French government) (grant to J.C.); French ministry of Defense (DGA) (to R.T.).

Notes

We thank Thomas Brochier, Nicolas Brunel, Gilles Laurent, Anders Ledberg, and William MacKay for critical comments to earlier versions of this work; Emmanuel Procyk and Martine Meunier for making available to use the MRI scanner facility (INSERM, Lyon, France); Thomas Brochier for generously sharing needed equipment; Andrea Brovelli, Lorenzo Guerrasio, and Florent Jaillet for help with data analysis; Ivan Balansard, Marc Martin, and Celine Mazenq for animal care; Joel Baurberg, Alain De Moya, and Xavier Degiovanni for technical assistance and the CORTEX software developers. *Conflict of Interest* : None declared.

References

Asher I, Stark E, Abeles M, Prut Y. 2007. Comparison of direction and object selectivity of local field potentials and single units in macaque posterior parietal cortex during prehension. J Neurophysiol. 97:3684–3695.

Baker SN, Kilner JM, Pinches EM, Lemon RN. 1999. The role of synchrony and oscillation in the motor output. Exp Brain Res. 128:109–117.

Batschelet E. 1981. Circular statistics in biology. London: Academic Press.

Berens P. 2009. CircStat: a Matlab toolbox for circular statistics [Internet]. J Stat Soft. 31. Available from: URL http://www.jstatsoft.org/v31/i10.

Brunel N, Wang XJ. 2003. What determines the frequency of fast network oscillations with irregular neural discharges? I. Synaptic dynamics and excitation-inhibition balance. J Neurophysiol. 90:415–430.
Buschman TJ, Miller EK. 2007. Top-down versus bottom-up control of attention in the prefrontal and posterior parietal cortices. Science. 315:1860–1862.
Buzsaki G. 2006. Rhythms of the brain. New York: Oxford University Press.
Conway BA, Halliday DM, Farmer SF, Shahani U, Maas P, Weir AI, Rosenberg JR. 1995. Synchronization between motor cortex and spinal motoneuronal pool during the performance of a maintained motor task in man. J Physiol. 489:917–924.
Coull JT, Nobre AC. 2008. Dissociating explicit timing from temporal expectation with fMRI. Curr Opin Neurobiol. 18:137–144.
Denker M, Roux S, Lindén H, Diesmann M, Riehle A, Grün S. 2011. The local field potential reflects surplus spike synchrony. Cereb Cortex. doi: 10.1093/cercor/bhr040.
Donoghue JP, Sanes JN, Hatsopoulos NG, Gaál G. 1998. Neural discharge and local field potential oscillations in primate motor cortex during voluntary movements. J Neurophysiol. 79:159–173.
Engel AK, Fries P. 2010. Beta-band oscillations—signalling the status quo? Curr Opin Neurobiol. 20:156–165.
Feng W, Havenith MN, Wang P, Singer W, Nikolić D. 2010. Frequencies of gamma/beta oscillations are stably tuned to stimulus properties. Neuroreport. 21:680–684.
Foffani G, Bianchi AM, Baselli G, Priori A. 2005. Movement-related frequency modulation of beta oscillatory activity in the human subthalamic nucleus. J Physiol. 568:699–711.
Gibbon J. 1977. Scalar expectancy theory and Weber's law in animal timing. Psychol Rev. 84:279–325.
Gieselmann MA, Thiele A. 2008. Comparison of spatial integration and surround suppression characteristics in spiking activity and the local field potential in macaque V1. Eur J Neurosci. 28:447–459.
Gross J, Schmitz F, Schnitzler I, Kessler K, Shapiro K, Hommel B, Schnitzler A. 2004. Modulation of long-range neural synchrony reflects temporal limitations of visual attention in humans. Proc Natl Acad Sci U S A. 101:13050–13055.
Guerrasio L, Quinet J, Büttner U, Goffart L. 2010. Fastigial oculomotor region and the control of foveation during fixation. J Neurophysiol. 103:1988–2001.
Heldman DA, Wang W, Chan SS, Moran DW. 2006. Local field potential spectral tuning in motor cortex during reaching. IEEE Trans Neural Syst Rehabil Eng. 14:180–183.
Hwang EJ, Andersen RA. 2009. Brain control of movement execution onset using local field potentials in posterior parietal cortex. J Neurosci. 29:14363–14370.
Jasper H, Penfield W. 1949. Electrocorticograms in man: effect of voluntary movement upon the electrical activity of the precentral gyrus. Arch Psychiatr Zeitschr Neurol. 83:163–174.
Jensen O, Goel P, Kopell N, Pohja M, Hari R, Ermentrout B. 2005. On the human sensorimotor-cortex beta rhythm: sources and modeling. Neuroimage. 26:347–355.
Kilavik BE, Confais J, Ponce-Alvarez A, Diesmann M, Riehle A. 2010. Evoked potentials in motor cortical local field potentials reflect task timing and behavioral performance. J Neurophysiol. 104:2338–2351.
Kilavik BE, Riehle A. 2010. Timing structures neuronal activity during preparation for action. In: Nobre AC, Coull JT, editors. Attention and time. Oxford: Oxford University Press. p. 257–271.
Kohonen T. 1997. Self-organizing maps. New York: Springer.
Kopell N, Ermentrout GB, Whittington MA, Traub RD. 2000. Gamma rhythms and beta rhythms have different synchronization properties. Proc Natl Acad Sci U S A. 97:1867–1872.
Kristeva R, Patino L, Omlor W. 2007. Beta-range cortical motor spectral power and corticomuscular coherence as a mechanism for effective corticospinal interaction during steady-state motor output. Neuroimage. 36:785–792.
Logothetis NK, Kayser C, Oeltermann A. 2007. In vivo measurement of cortical impedance spectrum in monkeys: implications for signal propagation. Neuron. 55:809–823.
Miller R. 2007. Theory of the normal waking EEG: from single neurones to waveforms in the alpha, beta and gamma frequency ranges. Int J Psychophysiol. 64:18–23.
Mitzdorf U. 1985. Current source-density method and application in cat cerebral cortex: investigation of evoked potentials and EEG phenomena. Physiol Rev. 65:37–100.
Murthy VN, Fetz EE. 1992. Coherent 25- to 35-Hz oscillations in the sensorimotor cortex of behaving monkeys. Proc Natl Acad Sci U S A. 89:5670–5674.
Murthy VN, Fetz EE. 1996. Oscillatory activity in sensorimotor cortex of awake monkeys: synchronization of local field potentials and relation to behavior. J Neurophysiol. 76:3949–3967.
Nauhaus I, Busse L, Carandini M, Ringach DL. 2009. Stimulus contrast modulates functional connectivity in visual cortex. Nat Neurosci. 12:70–76.
Neuper C, Pfurtscheller G. 2001. Evidence for distinct beta resonance frequencies in human EEG related to specific sensorimotor cortical areas. Clin Neurophysiol. 112:2084–2097.
Nicolelis MA, Ghazanfar AA, Stambaugh CR, Oliveira LM, Laubach M, Chapin JK, Nelson RJ, Kaas JH. 1998. Simultaneous encoding of tactile information by three primate cortical areas. Nat Neurosci. 1:621–630.
O'Leary JG, Hatsopoulos NG. 2006. Early visuomotor representations revealed from evoked local field potentials in motor and premotor cortical areas. J Neurophysiol. 96:1492–1506.
Panzeri S, Senatore R, Montemurro MA, Petersen RS. 2007. Correcting for the sampling bias problem in spike train information measures. J Neurophysiol. 98:1064–1072.
Pfurtscheller G, Neuper C, Pichler-Zalaudek K, Edlinger G, Lopes da Silva FH. 2000. Do brain oscillations of different frequencies indicate interaction between cortical areas in humans? Neurosci Lett. 286:66–68.
Pfurtscheller G, Stancák A, Jr, Neuper C. 1996. Post-movement beta synchronization. A correlate of an idling motor area? Electroencephalogr Clin Neurophysiol. 98:281–293.
Poulet JFA, Petersen CCH. 2008. Internal brain state regulates membrane potential synchrony in barrel cortex of behaving mice. Nature. 454:881–885.
Ray S, Maunsell JH. 2010. Differences in gamma frequencies across visual cortex restrict their possible use in computation. Neuron. 67:885–896.
Rickert J, Cardoso De Oliveira S, Vaadia E, Aertsen A, Rotter S, Mehring C. 2005. Encoding of movement direction in different frequency ranges of motor cortical local field potentials. J Neurosci. 25:8815–8824.
Saleh M, Reimer J, Penn R, Ojakangas CL, Hatsopoulos NG. 2010. Fast and slow oscillations in human primary motor cortex predict oncoming behaviorally relevant cues. Neuron. 65:461–471.
Sanes JN, Donoghue JP. 1993. Oscillations in local field potentials of the primate motor cortex during voluntary movement. Proc Natl Acad Sci U S A. 90:4470–4474.
Scherberger H, Jarvis MR, Andersen RA. 2005. Cortical local field potential encodes movement intention in the posterior parietal cortex. Neuron. 46:347–354.
Spinks RL, Kraskov A, Brochier T, Umilta MA, Lemon RN. 2008. Selectivity for grasp in local field potential and single neuron activity recorded simultaneously from M1 and F5 in the awake macaque monkey. J Neurosci. 28:10961–10971.
Stark E, Abeles M. 2007. Predicting movement from multiunit activity. J Neurosci. 27:8387–8394.
von Stein A, Sarnthein J. 2000. Different frequencies for different scales of cortical integration: from local gamma to long range alpha/theta synchronization. Int J Psychophysiol. 38:301–313.
Whittington MA, Traub RD, Kopell N, Ermentrout B, Buhl EH. 2000. Inhibition-based rhythms: experimental and mathematical observations on network dynamics. Int J Pschophysiol. 38:315–336.